

# Reclaiming High-Voltage APD Biases From Dropped Optical Data Signals of Multi-Lane Interconnects

Bernhard Schrenk, and Margareta V. Stephanie

AIT Austrian Institute of Technology, 1210 Vienna, Austria. [bernhard.schrenk@ait.ac.at](mailto:bernhard.schrenk@ait.ac.at)

**Abstract** As a method to extend the optical budget of intra-datacenter interconnects, we demonstrate the provision of a  $>20\text{V}$  APD bias through a shared energy reclamation circuit at the optical data plane. We find a penalty of  $0.2\text{ dB}$  with respect to electrically-supplied APDs. ©2022 The Author(s)

## Introduction

The continuous growth in datacenter information density is supported by switch cores with interconnect bandwidths that have recently surpassed  $10\text{ Tb/s}$  [1]. Various solutions are being investigated to support this growth in capacity in the optical communication domain, targeting an energy consumption in the  $\text{fJ/bit}$  range, electro-optic bandwidths of up to  $100\text{ GHz}$ , and ultra-small footprints [2]. As the scaling of symbol rates becomes increasingly challenging, simplified coherent approaches are now being considered for the very-short reach domain [3], while inverse multiplexing is explored under the context of massively-parallel interconnects. Towards the latter, micro-scale light emitting diodes have been demonstrated at  $2\text{ Gb/s/lane}$  in a  $16\times 16$  array configuration [4]. The introduction of APD-based reception in such multi-lane transmission links seems attractive as it would permit a higher optical budget. This provision of additional, unallocated budget can enable novel datacenter network architectures that go beyond the simple point-to-point layout that are mostly found for optical interconnects. However, the generation of APD biases of typically beyond  $20\text{V}$  necessitates electronic IC with high breakdown voltage. Such are not supported by nanometer-scale CMOS technology nodes that instead aim at a high degree of integration, high frequencies and a lower nominal supply voltage. The transistor voltage ratings scale down, which prevents their

ability to synthesize high-voltage circuits. This makes the efficient monolithic integration of high-bandwidth electronics with high-voltage photonic elements, such as APDs, difficult.

In this work, we take advantage of the fact that optical power is not “destroyed” during electro-optic data modulation but sunk to an unused circuit branch, where it can be reclaimed to generate an APD bias of  $>20\text{V}$ . We experimentally prove the extension of optical budget for a bidirectional 1-, 2- and 4-lane short-reach optical interconnect through APD-enabled reception sensitivities of  $-24.1\text{ dBm}$  at  $10\text{ Gb/s/lane}$  transmission. We confirm correct operation through a  $0.2\text{ dB}$  penalty with respect to an electrical APD bias supply.

## Optically Generated APD Bias

The proposed concept is sketched in Fig. 1 and relies on the scavenging of dropped optical power for the purpose of APD bias generation in a bidirectional multi-lane communication link. One possibility to do so is to locally collect the dropped light modulation at the “dead” port of an interferometric modulator through a photovoltaic ladder, as introduced in Fig. 1a. In contrast to earlier works on optical energy harvesting [5–10], which mainly targeted the provision of high supply currents for low-voltage actuation of devices such as MOEMS switches, APDs require the supply of a high bias voltage at a rather low photocurrent. Moreover, the proposed scheme re-uses light that is extinct by optical

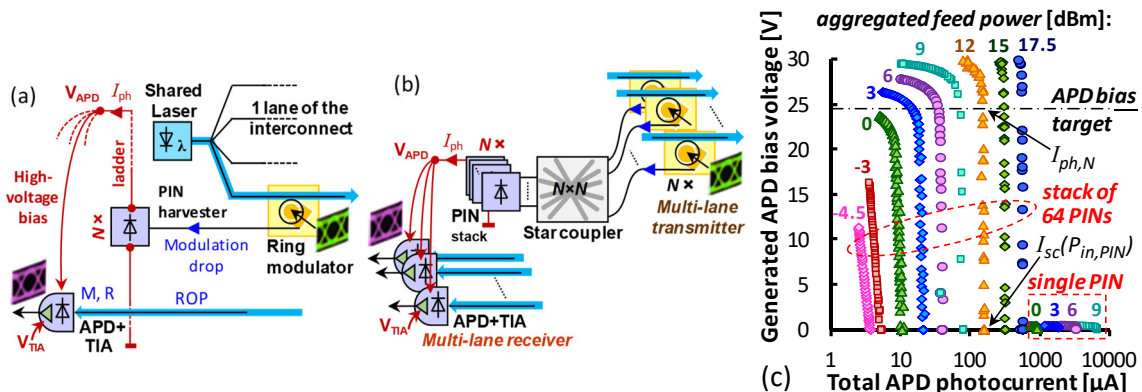
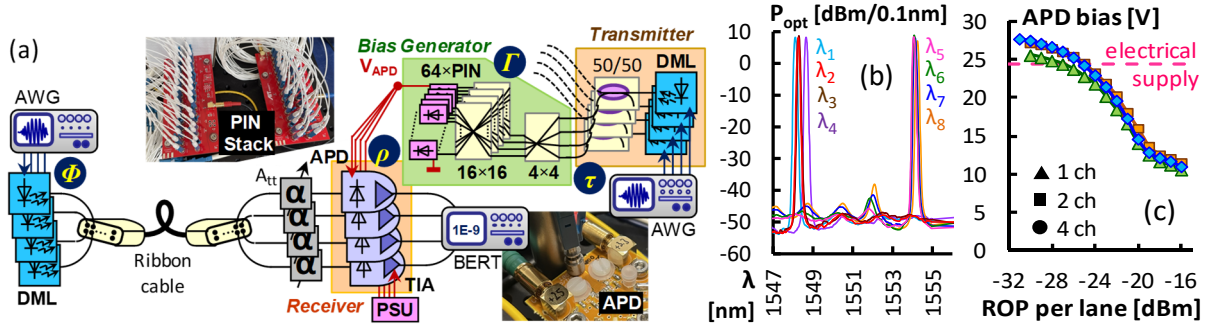


Fig. 1: Optically generated APD bias through (a) PIN ladder or (b) feed network. (c) V-I characteristics of generated bias.



**Fig. 2:** (a) Experimental setup. (b) Optical emission spectra for the two sets of four DMLs. (c) Optically generated APD bias.

intensity modulators during space bits – light that would be left unexplored.

By aggregating and converting the dropped optical power over multiple serialized PIN diodes operated in photovoltaic mode, a high voltage can be generated, as we will prove shortly. Moreover, this APD bias can be established without entering a regime that basically prevents the supply of a photocurrent  $I_{ph}$  generated by the received optical data signals at a received optical power (ROP) impinging onto multiple APDs. For example,  $N$  APDs operating at a responsivity of  $R = 1$  A/W and a multiplication factor of  $M = 10$  would lead to a photocurrent of  $I_{ph} = N \cdot R \cdot M \cdot ROP = N \cdot 32 \mu A$  for a ROP of  $-25$  dBm. It is important to note the dependence of  $M$  on the bias  $V_{apd}$ . Therefore, the drain of a higher photocurrent  $I_{ph}$  for a high ROP will inevitably lead to a drop in  $V_{apd}$  and, accordingly, a BER increase due to a reduced  $M$ . This limits the dynamic range that can be accomplished when employing optically biased APD receivers.

Since the experiment in this work was not able to build on a plethora of  $N$  ring modulators, a slightly different scavenging method is adopted (Fig. 1b). Rather than dedicating a modulator drop port to a single photovoltaic PIN harvester, the drop ports of  $N$  data transmitters operating at a generally random wavelength are shared among  $N$  PIN harvesters by means of passive star coupling. This is roughly equivalent to the previous case since  $N$  dropped data signals feed a single PIN diode, yet after passing the loss of an  $N \times N$  split. The proposed optical bias generator is shared among multiple lanes and can thus be implemented in a very compact way since neither star couplers nor photodiodes require a large footprint [11, 12].

Given the nature of continuous data transfer between the endpoints of the multi-lane link, the scavenged APD bias and the associated APD photocurrent have to be supplied continuously. The energy harvester can therefore not accumulate and store energy in a reservoir for sporadic actuation of optical switches or other latching photonic elements [5-7, 9, 10].

Figure 1c reports on the harvesting efficiency

to generate an APD bias with a target of 24.5V. Shown are the V-I relation under load, as they are characteristic for a photovoltaic supply. Results are presented as function of the aggregated optical power (that would be dropped at the modulators of all lanes) feeding the reclamation circuit. The set bias target can be reached for a feed of 3 dBm, however, the permissible photocurrent for all lanes is then only 15  $\mu A$ . This current  $I_{ph,N}$  is closely related to the short-circuit current  $I_{sc}$  (Fig. 1c), which is given by the optical power  $P_{in,PIN}$  arriving at a PIN element of the energy harvester.

Given for example the 4 lanes used in the present experiment and a ROP of  $-25$  dBm for signal reception at low BER, a photocurrent of 126  $\mu A$  would have to be supplied. For this, a feed power of slightly less than 12 dBm is required, corresponding to a dropped power of  $\sim 6$  dBm per modulator. The provision of the photocurrent for the given implementation of the energy reclamation circuit will also determine the dynamic range for signal reception, as will be discussed shortly. It shall also be underscored that the passive star coupler preceding the PIN stack represents a wavelength-agnostic feed distribution network that operates independently of the transmitter wavelengths. This, however, leads to the highest signal distribution loss and thus limits the accomplishable  $P_{in,PIN}$  and the permissible photocurrent  $I_{ph,N}$ . In case that the communication lanes should adopt CWDM, a similar approach can be followed for the feed distribution network, thus greatly increasing  $I_{ph,N}$  while reducing the required feed power.

For comparison, Fig. 1c also presents the V-I characteristics of a single PIN photodiode. The generated voltage under no load is 0.55V, while currents beyond 1 mA can be accomplished due to the absence of the 64-way split.

### Experimental Multi-Lane Interconnect

Figure 2a presents the experimental setup that resembles a bidirectional interconnect. Based on the availability of high-speed directly modulated lasers (DML), up to 4 lanes have

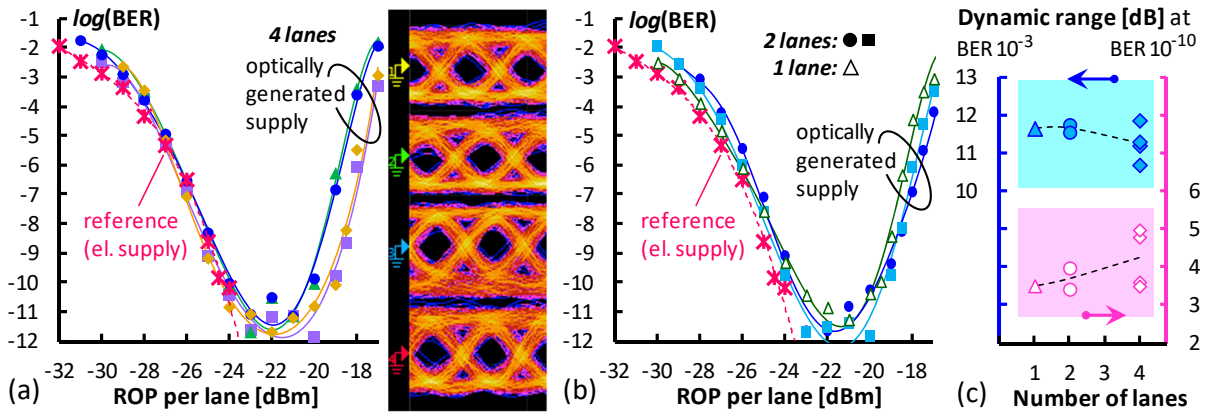


Fig. 3: BER performance for (a) 4-lane and (b) 2- and 1-lane link with optical APD bias generation. (c) Dynamic range.

been implemented. Two sets of four DMLs at  $\sim 1550$  nm (Fig. 2b), featuring a launch power of 10 dBm, have been employed as 10 Gb/s transmitters in either direction. The transmitter configuration ( $\tau$ ) is chosen in a way that an additional 50/50 coupler appended to the DML emulates the function of an externally-sourced micro-ring modulator, which drops the extinct light output to the APD bias generator ( $J$ ). For the latter, a  $64 \times 64$  configuration with 64 photovoltaic PIN diodes has been chosen. The average insertion loss over the compound  $4 \times 4 + 16 \times 16$  stage was 19.7 dB. The scavenged modulation drop is converted to a high bias  $V_{\text{apd}}$ , which supplies the photodiodes of four APDs at the receiver ( $\rho$ ), whereas the corresponding TIA is supplied by a local 3.3V rail. The commercial 10G APDs were rated for a typical sensitivity of -25.5 dBm. The 10 Gb/s data signals at the far end of the lanes ( $\phi$ ) are fed over a short ribbon cable and delivered to the APD+TIA receivers. This allows an investigation of the overload conditions of the bias generator for higher received power levels. Finally, the transmission performance as function of the ROP is acquired through real-time BER testing.

## Results and Discussion

The generated APD bias for a 1-, 2- and 4-lane configuration is presented in Fig. 2c. The APD bias is rather independent of the number of lanes: the beneficial increase in feed power is eroded by the provision of an equally increased aggregated APD photocurrent. It falls below 15V for a ROP of about -20 dBm as the total photocurrent cannot be longer sustained. The slightly worse performance of the 1-lane link ( $\blacktriangle$ ) is explained by unfortunate excess loss of the feeding channel within the power splitting network that feeds the PIN stack of the energy harvester, and the missing ability to average out excess loss due to the single feed channel.

Figure 3b shows the BER performance for a 4-lane interconnect. For an electrically supplied

APD bias the reception sensitivity was -24.3 dBm ( $\times$ ). The penalty was 0.2 dB when instead using the energy reclamation circuit to supply the 4 APDs ( $\blacktriangle, \bullet, \blacksquare, \blacklozenge$ ). The correct operation is further evidenced by the eye diagrams that have been appended to Fig. 3b. However, due to the aforementioned drop in APD bias for a higher ROP, the dynamic range is limited: The BER of  $10^{-10}$  is surpassed at an increased ROP of -20.3 dBm ( $\blacktriangle, \bullet$ ), limiting the dynamic range to 3.6 dB. However, this reflects the current situation in intra-datacenter links, whose dynamic range is restricted by an already low optical budget of up to  $\sim 6$  dB, while for the current scheme the same optical budget can be significantly boosted to  $\sim 28$  dB at 10 Gb/s by virtue of the APD gain.

Figure 3c reports the BER for a 1- ( $\triangle$ ) and 2-lane ( $\bullet, \blacksquare$ ) interconnect. The reception sensitivities were -23.7 and -23.3 dBm, respectively, and thus remained within a 1-dB range. The dynamic range for all lanes is summarized in Fig. 3d for all three link configurations and two reference BER levels. As for the reception sensitivity, we found a performance that is widely independent of the number of communication lanes.

## Conclusions

We have experimentally evaluated the generation of an APD bias of  $\sim 25$ V by means of shared (up to 64 lanes) photovoltaic power conversion circuit for locally dropped optical data signals. We showed a negligible penalty (0.2 dB) with respect to electrically biased APD receivers, with sensitivities (-24.1 dBm at 10 Gb/s/lane, 4 lanes) being widely independent on the number of communication lanes. The APD-enabled improvement in sensitivity can be beneficially used to extend the loss budget while unleashing new datacenter architectures. The present limitation in dynamic range (4.2 dB) requires a re-design for the energy reclamation circuit towards driving a higher photocurrent, as associated with higher ROP levels.

## Acknowledgements

This work was supported by the ERC under the EU Horizon-2020 programme (grant n° 804769) and by the Austrian FFG agency through the JOLLYBEE project (grant n° FO999887467).

## References

- [1] A. Agrawal, and C. Kim, "Intel Tofino2 – A 12.9Tbps P4-Programmable Ethernet Switch," in *Proc. 2020 IEEE Hot Chips 32 Symposium (HCS)*, 2020, DOI: 10.1109/HCS49909.2020.9220636.
- [2] C. Thraskias, E. Lallas, N. Neumann, L. Schares, B. Offrein, R. Henker, D. Plettemeier, F. Ellinger, J. Leuthold, and I. Tomkos, "Survey of Photonic and Plasmonic Interconnect Technologies for Intra-Datacenter and High-Performance Computing Communications," *IEEE Communications Surveys & Tutorials*, vol. 20, no. 4, pp. 2758-2783, Fourthquarter 2018, DOI: 10.1109/COMST.2018.2839672.
- [3] B. Buscaino, B. D. Taylor, and J. M. Kahn, "Multi-Tb/s-per-Fiber Coherent Co-packaged Optical Interfaces for Data Center Switches," *Journal of Lightwave Technology*, vol. 37, no. 13, pp. 3401-3412, Jul. 2019, DOI: 10.1109/JLT.2019.2916988.
- [4] B. Pezeshki, F. Khoeini, A. Tselikov, R. Kalman, C. Danesh, and E. Afifi, "MicroLED Array-based Optical Links Using Imaging Fiber for Chip-to-chip Communications," in *Proc. Optical Fiber Communication Conference (OFC)*, 2022, San Diego, United States, paper W1E.1. DOI: 10.1364/OFC.2022.W1E.1.
- [5] Y. Bi, J. Jin, A.R. Dhaini, and L.G. Kazovsky, "QPAR: A Quasi-Passive Reconfigurable Green Node for Dynamic Resource Management in Optical Access Networks," *Journal of Lightwave Technology*, vol. 32, no. 6, pp. 1104-1115, 2014, DOI: 10.1109/JLT.2013.2296052.
- [6] B. Schrenk, R. Lieger, T. Lorünser, P. Bakopoulos, A. Poppe, M. Stierle, H. Avramopoulos, and H. Leopold, "Fully-Passive Resiliency Node for Optical Access," *Journal of Optical Communications and Networking*, vol. 7, no. 11, pp. 10-15, 2015, DOI: 10.1364/JOCN.7.000B10.
- [7] B. Schrenk, F. Laudenbach, R. Lieger, T. Lorünser, P. Bakopoulos, A. Poppe, M. Stierle, H. Avramopoulos, and H. Leopold, "Passive ROADM Flexibility in Optical Access with Spectral and Spatial Reconfigurability," *Journal on Selected Areas in Communications*, vol. 33, no. 12, pp. 2837-2846, 2015, DOI: 10.1109/JSAC.2015.2478719.
- [8] T. Umezawa, A. Kanno, P.T. Dat, K. Akahane, Y. Awaji, N. Yama, N. Yamamoto, and T. Kawanishi, "Multi-Core Based 94-GHz Radio and Power over Fiber Transmission Using 100-GHz Analog Photoreceiver," in *Proc. European Conference on Optical Communication (ECOC)*, 2016, Dusseldorf, Germany, paper Th.2.P2.SC7.2.
- [9] P. Iannone, A.H. Gnauck, M. Straub, J. Hehmann, L. Jentsch, T. Pfeiffer, and M. Earnshaw, "An 8- × 10-Gb/s 42-km High-Split TWDM PON Featuring Distributed Raman Amplification and a Remotely Powered Intelligent Splitter," *Journal of Lightwave Technology*, vol. 35, no. 7, pp. 1328-1332, 2017, DOI: 10.1109/JLT.2017.2654967.
- [10] M. Straub, L. Jentsch, J. Hehmann, T. Pfeiffer, and R. Bonk, "Remotely Powered Inline OTDR Unit with Unique Identification Possibility of Power Splitter Branches for Use in Access Network Applications," in *Proc. European Conference on Optical Communication (ECOC)*, 2018, Rome, Italy, paper We2.68, DOI: 10.1109/ECOC.2018.8535122.
- [11] P.D. Trinh, S. Yegnanarayanan, and B. Jalali, "5x9 Integrated Optical Star Coupler in Silicon-on-Insulator Technology," *Photonics Technology Letters*, vol. 8, no. 6, pp. 794-796, Jun. 1996, DOI: 10.1109/68.502097.
- [12] G.B. Cao, L.J. Dai, Y.J. Wang, J. Jiang, H. Yang, and F. Zhang, "Compact Integrated Star Coupler on Silicon-on-Insulator," *Photonics Technology Letters*, vol. 17, no. 12, pp. 2616-2618, Dec. 2005, DOI: 10.1109/LPT.2005.859408.